The Localized Microwave-Heating (LMH) Paradigm – Theory, Experiments, and Applications

Yehuda Meir and Eli Jerby*

Faculty of Engineering, Tel Aviv University, Ramat Aviv, 69978, Israel.

ABSTRACT

This paper introduces the localized microwave heating (LMH) concept, based on the intentionally induced thermal-runaway instability, and reviews its various applications in a unified approach. The theory and experiments of hotspot formation in various materials, including glass and metal powders, are presented. Recent developments of applications based on LMH effects are reviewed. The concept is extended beyond microwave drills to miniature microwave heaters for other applications including for instance (a) plasma ejection from hotspots as a means for nano-powder production from solids, (b) ignition of thermite reactions for material processing and combustion, (c) local sintering of metal powders, and (d) material identification by breakdown spectroscopy. The potentials and limitations of LMH as a low-cost laser substitute in various applications are discussed.

INTRODUCTION

Microwave heating is performed volumetrically in most cases, in ovens, applicators, and furnaces, with a typical heat-affected zone (HAZ) comparable to the microwave wavelength, in the order of ~0.1 m or larger [1, 2]. As an exception, the microwave drill [3] utilizes the induced thermal-runaway mechanism [4] which enables a sub-wavelength HAZ in the order of ~10^{-3} m. The localized microwave heating (LMH) effect, embodied in the microwave-drill mechanism, can be used for a variety of other applications as presented here in a generalized approach.

LMH may occur in materials possessing temperature-dependent properties that dictate faster energy absorption than diffusion rate [5]. The LMH instability is ceased at the material's phase transition, to liquid, gas or plasma. The HAZ size is determined by the material's properties, the microwave wavelength and power, and by the applicator geometry. LMH effects were demonstrated by microwave drills in various materials such as concrete, ceramics, basalts, glass, polymers, and silicon [6-12]. A doping effect induced by LMH in silicon is presented in [13]. LMH is studied also for medical applications such as tissue heating [14], bone drilling [15], interstitial treatments [16, 17], and ablation for cancer therapy [18]. Open-end coaxial applicators are used also for direct heating of liquid by microwave radiation [19] and for activation of chemical reactions [20]. LMH may generate also plasmoids and fireball directly from solid substrates [21, 22] and produce nano-particles [23-25].

This paper presents the LMH paradigm, including its theoretical and experimental studies in dielectric solids and metal powders, and discusses in a unified approach new LMH applications emerged recently.

* Corresponding author: jerby@eng.tau.ac.il

LMH MODEL

The LMH model [4], extended to include magnetic heating effects [26], consists of the EM-wave and heat equations,

$$\nabla\times\left[\left(\mu_r'-j\mu_r''\right)^{-1}\nabla\times\tilde{\mathbf{E}}\right]-\left[\varepsilon_r'-j\left(\varepsilon_r''+\sigma/\omega\varepsilon_0\right)\right]k_0^2\tilde{\mathbf{E}}=0\,, \tag{1}$$

$$\rho c_p\,\partial T/\partial t-\nabla\cdot\left(k_{th}\nabla T\right)=Q_d\,, \tag{2}$$

coupled by the EM-heat dissipation,

$$Q_d=\frac{1}{2}\left[\left(\sigma+\omega\varepsilon_0\varepsilon_r''\right)\left|\tilde{\mathbf{E}}\right|^2+\omega\mu_0\mu_r''\left|\tilde{\mathbf{H}}\right|^2\right], \tag{3}$$

and by the temperature-dependent material properties, $\varepsilon(T)$, $\mu(T)$, $\sigma(T)$, $k_{th}(T)$, $\rho c_p(T)$ (namely the permittivity and permeability, the electric and thermal conductivities, the density and heat capacity, respectively) where $\tilde{\mathbf{H}}=j\left(\omega\mu_0\mu_r\right)^{-1}\nabla\times\tilde{\mathbf{E}}$. The temperature T is varying slowly with respect to the EM wave, hence the distinction between the typical time scales of the EM wave propagation (~1 ns) and the much slower thermal evolution (>1 ms) allows the *two-time scale* approximation. Its validity is verified by the heuristic condition $\rho c_p d_{hs}^2/k_{th}\gg\tau$, where d_{hs} is the hotspot width and $\tau=2\pi/\omega$ is the wave period. The EM bandwidth is sufficiently narrow to neglect parametric variation with frequency, hence the wave equation (1) is solved in the frequency domain while the heat equation (2) is computed in the slowly-varying time domain.

The LMH instability can be explained in a figurative manner as shown in Fig. 1. The open-end applicator is applied to a material of which the dielectric loss factor tends to increase and the thermal conductivity tends to decrease with temperature. The initial heating of the (initially) uniform material increases the temperature near the electrode tip, hence the spatial distributions of the material properties vary accordingly. The loss factor increases (and the thermal conductivity decreases) in this vicinity, hence more and more power is absorbed there, which leads to an unstable LMH response.

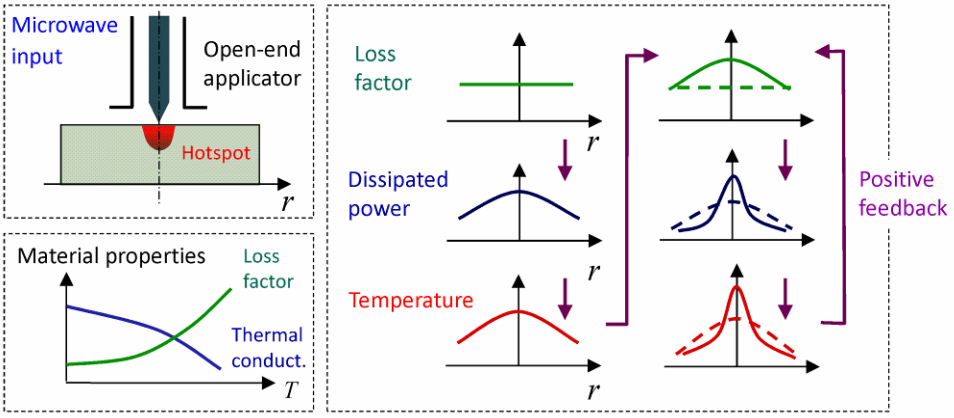

Fig. 1: The induced thermal-runaway instability and self-focusing effects illustrated [4].

The nonlinear LMH effect is simulated by a numerical solution of Eqs. (1-3) using Comsol Multiphysics® with known temperature-dependent material properties.

DIELECTRIC LMH

The dielectric LMH effect is demonstrated here by applying 100-W microwave power locally into a 1-mm thick soda-lime glass plate. The numerical results presented in Figs. 2a, b show the hotspot formation by the temperature elevation, by the HAZ full-width half maximum (FWHM) evolution in time, and by the spatial temperature profile in the vicinity of the electrode tip. The turning point of the heating rate in Fig. 2a, associated with a relative shrinking of the hotspot, marks the thermal-runaway instability. The electric field is enhanced near the electrode tip hence the EM-energy is self focused there.

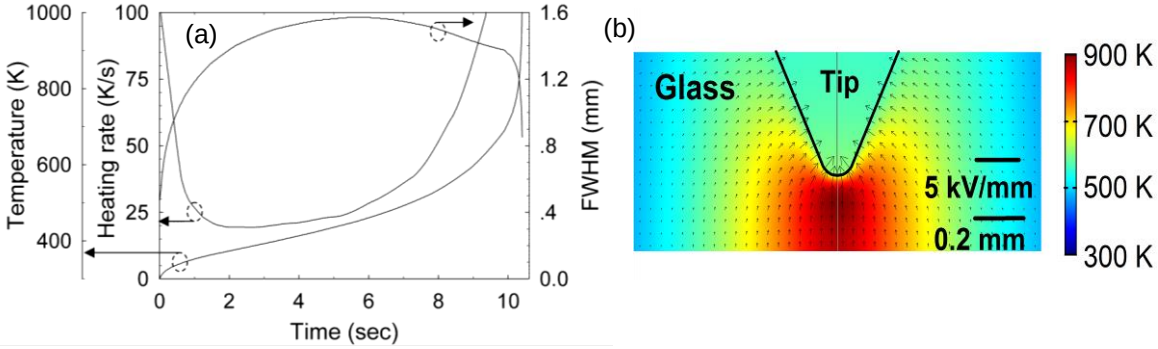

Fig. 2: Simulation results of the temperature and HAZ evolution (a) and the spatial distributions of the temperature and electric field in the hotspot at 900K (b).

The experimental setup employs a solid-state applicator as in [27] with a FLIR SC302 thermal camera directed in a 45° view to the upper surface. Figure 3 shows the temperature spatial evolution measured by the thermal camera (a), the final thermal image obtained (b) and the consequent modification of the glass shape (c). The experimental results reasonably agree with the simulation.

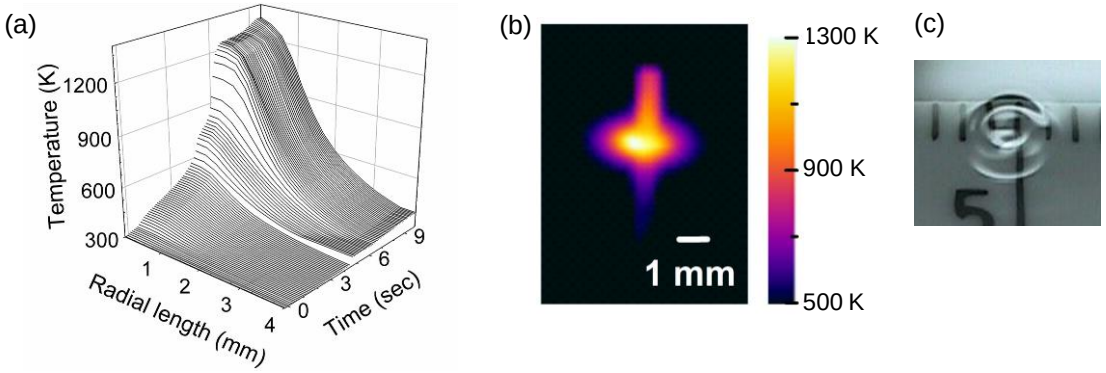

Fig. 3: LMH experiments in glass; (a) the HAZ evolution measured by the thermal camera, (b) the final thermal image, and (c) the resulted modified surface shape.

The hotspot confinement, its time-to-melt (TTM) and final size depend on the microwave power applied. Table I shows simulation results for 100 and 200 W and the significant impact of the power increase on the TTM shortening, the hotspot size shrinking, and the total energy reduction. Hence the LMH is more effective in shorter exposure times to higher microwave power levels, in general.

Table I: The microwave-power effect on the time-to-melt, hotspot size, and total energy.

Microwave power (kW)	Time to melt (s)	Hotspot size (mm)	Total energy (kJ)
0.1	10	1.6	1
0.2	2	1.1	0.4

MAGNETIC LMH

Recent experiments show that metal powders with negligible dielectric losses can be heated effectively by LMH [28]. This effect is attributed to the magnetic component of the EM field and the eddy currents evolved in the metal-powder particles. Figure 4 shows simulation results of an open-end applicator immersed in a copper powder. The temperature dependent properties of the copper powder were found using Ref. [29]. The location of the maximal temperature in Fig. 4a indicates the dominance of the magnetic heating. This model is valid up to the necking temperature of the copper particles.

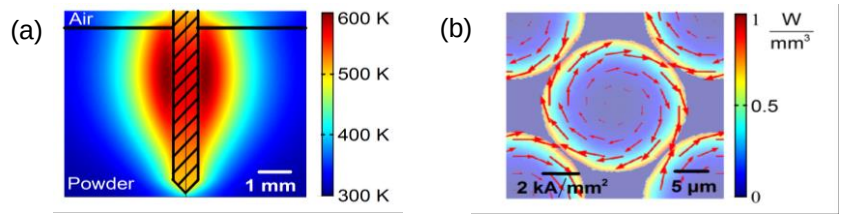

Fig. 4: LMH simulation of copper powder; (a) the temperature distribution around the tip, and (b) the eddy currents induced by the magnetic-field component [28].

The magnetic LMH was demonstrated experimentally by applying the setup presented above to copper powder (DirectMetal-20). The center electrode of the open-end applicator was inserted 6 mm into the copper powder as in Fig. 4a. Figure 5a presents the evolution of the HAZ temperature profile measured by the thermal camera, and Figs. 5b, c show its comparison to the magnetic LMH model. The LMH effect is not characterized by thermal-runaway instability in this case since the temperature tends to stabilize at ~700 K due to the powder particle necking and consolidation effects.

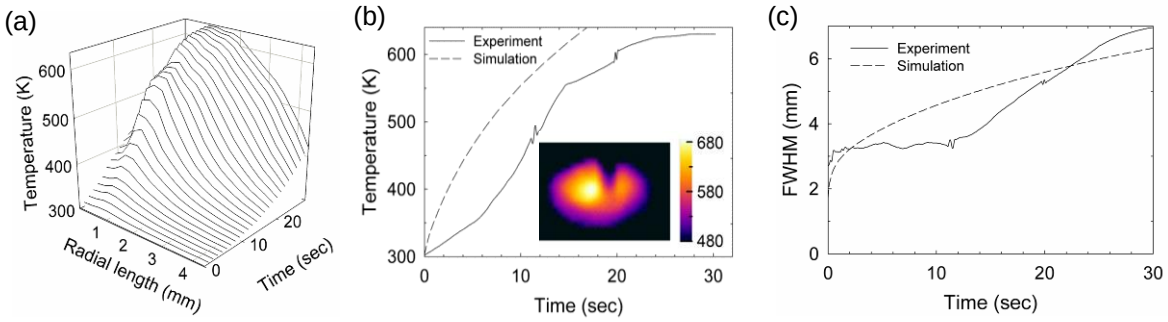

Fig. 5: Experimental demonstration of magnetic LMH in metal powder. The hotspot evolution measured by a thermal camera (a), compared to the simulated temperature (b) and HAZ size (c).

PLASMA GENERATION BY LMH

Plasma, in forms of fireball and fire-column, can be ejected by LMH directly from solid or liquid substrates (including metals) as presented in Refs. [21-25]. The LMH process begins by a hotspot formation (Fig. 6a) as presented above, but for plasma ejection the electrode is lifted up to detach the molten drop from the surface and to form a buoyant fireball (Fig. 6b). Beside their resemblance to natural ball-lightning phenomena, these fireballs may have practical importance due to the nano-particles produced directly from the substrate material as shown in Fig. 6c.

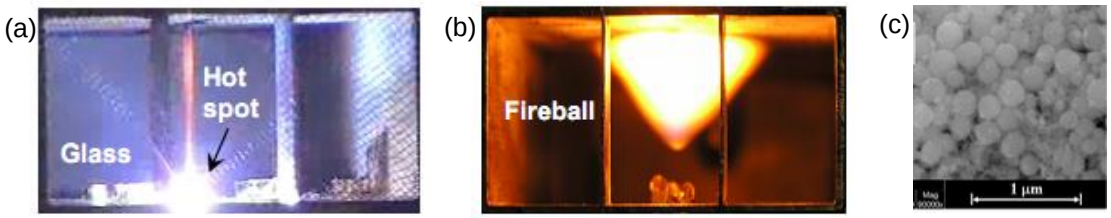

Fig. 6: Plasmoid ejection from glass; (a) a hotspot created by LMH, (b) a fireball emitted to the microwave cavity, and (c) nano-particles produced in the process [25].

The plasma generated by LMH can be used also for material identification [30]. Similarly to the laser induced breakdown spectroscopy (LIBS), the material is identified by atomic emission spectroscopy of the light emitted by the plasma ejected from the hotspot. Figure 7a shows optical spectrum emitted by LMH of copper. The distinction between copper, aluminum and silicon in Fig. 7b demonstrates the feasibility of the LMH identification concept, namely the microwave-induced breakdown spectroscopy (MIBS).

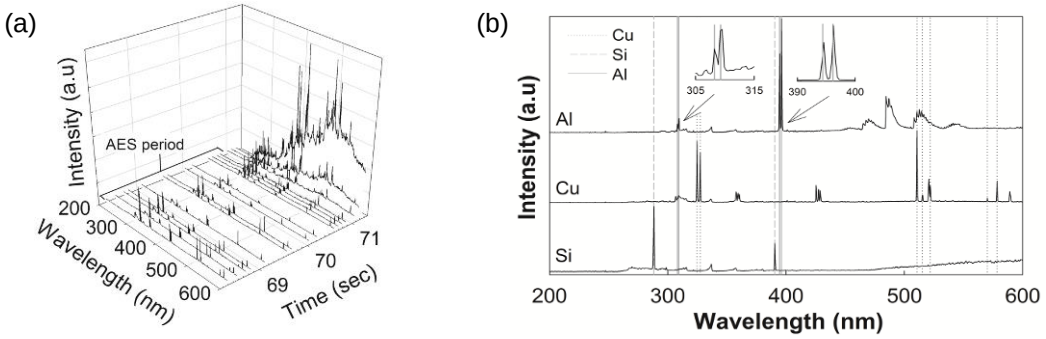

Fig. 7: Material identification by LMH plasma; (a) temporal evolution of copper optical spectrum under LMH, and (b) the distinction between aluminum, copper and silicon lines [30].

THERMITE IGNITION BY LMH

Ignition of thermite reactions in powder mixtures of pure aluminum and magnetite (or hematite) was found recently to be doable by LMH [26]. The initiation of this exothermic reaction by the LMH demonstrates an example for local ignition of various high-temperature self-propagating syntheses (SHS). The thermite mixture has both dielectric and magnetic loss factors. The magnetic LMH is implemented by a short-end applicator to enhance the magnetic field in front of it. It achieves a faster heating rate than the open-end dielectric LMH up to the Curie temperature at 858K where the magnetic loss

significantly dereases. Integrating electrical LMH enables the thermal-runaway instability and the thermite ignition as shown in Figs. 8a, b. The required microwave pulse duration for ignition, shown in Fig. 8c, carries less energy at higher power rates. The experiments demonstrate also the feasibility of cutting and welding by relatively low-power LMH.

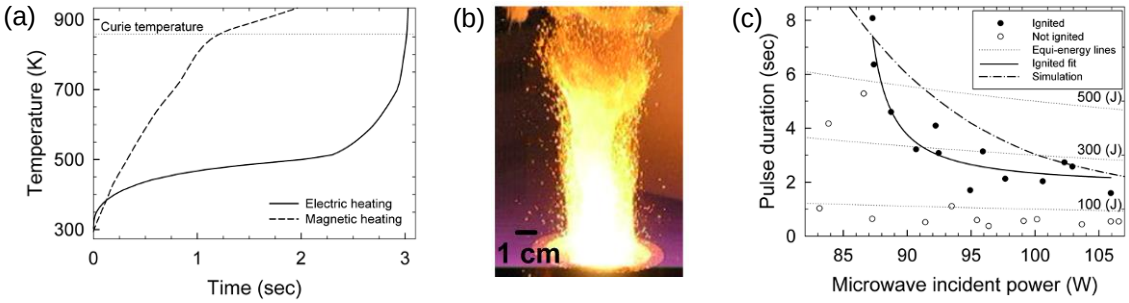

Fig. 8: Thermite ignition by LMH; (a) simulation of magnetic and dielectric heating, (b) the thermite flame, and (c) the microwave power required for LMH ignition [27].

LOCAL SINTERING BY LMH

The LMH effect in metal powders, associated with internal plasma breakdowns between the particles, leads to local melting and solidification of the metal powder, as shown in Fig. 9a. We study this effect in collaboration with ASCAMM, Barcelona, as a potential technique for a stepwise 3D construction [28]. The consolidated drop can be placed, as a building block, on top of previously constructed structure in a process of additive manufacturing, as illustrated Fig. 9b.

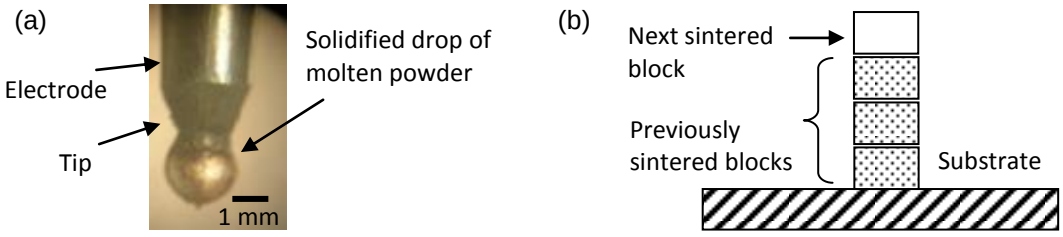

Fig. 9: Localized solidification of metal powder by LMH [28]; the electrode functions as a pickup for the solidified metal sphere (a) in a stepwise additive process (b).

SURFACE TREATMENT AND DOPING BY LMH

A recent study shows the feasibility of local doping of silicon by silver and aluminum using LMH [13]. The dopant material in these experiments, incorporated in the electrode tip, is diffused into the locally heated bulk and forms a sub-micron junction. The doping depth depends on the applied microwave power. Oxidation effects are also observed in these experiments conducted in air atmosphere. Chemical reactions applied by LMH for surface treatment may include also thermite reactions [26] for rust conversion to iron. These LMH techniques open new possibilities for a variety of surface treatments and local surface processing.

CONCLUSIONS

The LMH paradigm presented in this paper extends the common microwave-heating technology to HAZ sizes much smaller than the microwave wavelength. In LMH, the microwave radiation is self-focused intentionally within a millimeter-size hotspot hence melting or evaporating it locally. By the electrode manipulation, dusty plasma rich with nanoparticles can be ejected directly from the substrate.

The LMH does not require a cavity or a closed chamber, and it can be implemented by conventional low-cost microwave generators. In the low-power range, LMH can be implemented even by a solid-state generator [27]. The LMH paradigm incorporates the theory of the induced thermal-runaway instability [4] (extended to include magnetic heating) and experimental studies of local melting and plasma ejection effects. The LMH is applicable to dielectrics and metals as well, in solid, powder, and liquid forms. Figure 10 shows a conceptual scheme of the LMH relevance to matter states and their transitions, and some of the applications related to them.

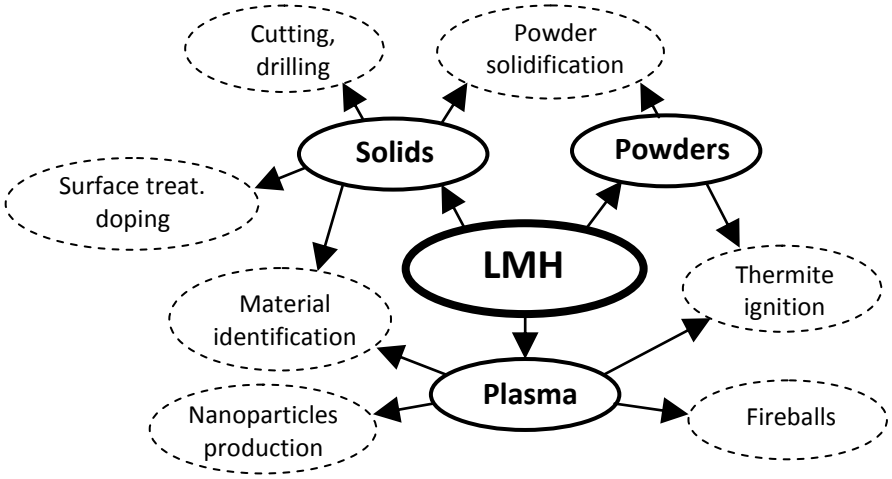

Fig. 10: LMH relevance to matter states and transitions, and their related applications.

The LMH technique can be considered as a partial substitute for some laser-based applications (e.g. drilling, cutting, joining, surface treatment, material identification, rapid manufacturing) to a limited extent. While LMH may provide low-cost and compact solutions in this regard, it requires a physical contact with the object and its ~1mm resolution is inferior with respect to lasers. It is expected therefore that LMH will find applications in ranges of larger volumes and rougher missions, as a complementary means to the relatively more accurate and expensive lasers.

REFERNCES

1. A. C. Metaxas, *Foundations of Electroheat: A Unified Approach*, John Wiley & Sons Ltd., Chichester, 1996.
2. S. Chandrasekaran, S. Ramanathan, T. Basak, *AIChE Journal* **58**, 330 (2012).
3. E. Jerby, V. Dikhtyar, O. Aktushev, U. Grosglick, *Science* **298**, 587 (2002).
4. E. Jerby, O. Aktushev, V. Dikhtyar, *Jour. Appl. Phys.* **97**, 034909 (2005).
5. Y. Alpert, E. Jerby, *IEEE Trans. Plasma Sci.* **27**, 555 (1999).

6. E. Jerby, V. Dikhtyar, *Advances in Microwave and Radio-Frequency Processing*, M. Willert-Porada (Ed.), Springer, 2006.
7. E. Jerby, O. Aktushev, V. Dikhtyar, P. Livshits, A. Anaton, T. Yacoby, A. Flax, A. Inberg, D. Armoni, *Microwave and Radio-Frequency Applications 4th World Congress*, Conf. Proc., pp. 156-165, Austin, Texas, Nov. 4-7, 2004.
8. E. Jerby, V. Dikhtyar, O. Aktushev, *Amer. Ceramic Soc. Bulletin* **82**, 35 (2003).
9. X. Wang, W. Liu, H. Zhang, S. Liu, Z. Gan, *7th Int'l Conf. Electronics Packaging Technology*, Proc. Article # 4198945, Aug. 26-29, 2006, Shanghai, China.
10. E. Jerby, A.M. Thompson, *Jour. Amer. Ceram. Soc.* **87**, 308 (2004).
11. J. B. A. Mitchell, E. Jerby, Y. Shamir, Y. Meir, J. L. LeGarrec, M. Sztucki, *Polym. Degradation Stab.* **96**, 1788 (2011).
12. R. Herskowits, P. Livshits, S. Stepanov, O. Aktushev, S. Ruschin, E. Jerby, *Semicond. Sci. Technol.* **22**, 863 (2007).
13. P. Livshits, V. Dikhtyar, A. Inberg, A. Shahadi, E. Jerby, *Microelectron. Eng.* **88**, 2831 (2011).
14. A. Copty, F. Sakran, M. Golosovsky, D. Davidov, *Appl. Phys. Lett*. **24**, 5109 (2004).
15. Y. Eshet, R. Mann, A. Anaton, T. Yacoby, A. Gefen, E. Jerby, *IEEE Trans. Biomedical Eng.* **53**, 1174 (2006).
16. T. Z. Wong, B. S. Trembly, *Int. J. Radiat. Oncol. Biol. Phys.* **28**, 673 (1994).
17. I. Longo, G. B. Gentili, M. Cerretelli, N. Tosoratti, *IEEE Trans. Biomed. Eng*. **50**, 82 (2003).
18. C. L. Brace, *Curr. Probl. Diagn. Radiol.* **38**, 61 (2009).
19. G. B. Gentili, M. Linari, I. Longo, A. S. Ricci, *IEEE Trans. Microwave Theory Tech.* **57**, 2268 (2009).
20. I. Longo, A. S. Ricci, *J. Microw. Power Electromagn. Energy* **41**, 1 (2007).
21. V. Dikhtyar, E. Jerby, *Phys. Rev. Lett.* **96**, 045002 (2006).
22. E. Jerby, *IEEE Trans. Plasma Sci*. **39**, 2198 (2011).
23. J.B.A. Mitchell, J.L. LeGarrec, M. Sztucki, T. Narayanan, V. Dikhtyar, E. Jerby, *Phys. Rev. Lett.* **100**, 065001 (2008).
24. E. Jerby, A. Golts, Y. Shamir, S. Wonde, J. B. A. Mitchell, J. L. LeGarrec, T. Narayanan, M. Sztucki, D. Ashkenazi, Z. Barkay, *Appl. Phys. Lett.* **95**, 191501 (2009).
25. E. Jerby, O. Meshcheryakov, D. Ashkenazi, Z. Barkay, N. Eliaz, J. B. A. Mitchell, T. Narayanan, J. L. LeGarrec, M. Sztucki, S. Wonde, *Proc. Ampere 13th Int'l Conf.*, pp. 383-386, Sept. 5-8, 2011, Toulouse, France.
26. Y. Meir, E. Jerby, *Combust. Flame* **159**, 2474 (2012).
27. Y. Meir, E. Jerby, *IEEE Trans. Microwave Theory Tech.* **60**, 2665 (2012).
28. A. Salzberg, E. Jerby, Y. Meir, X. Planta, B. Cavallini, J. Ardanuy, submitted to the *Journal of Materials Processing Technology*.
29. T. Galek, K. Porath, E. Burkel, U. Rienen, *Modell. Simul. Mater. Sci. Eng.* **18**, 025015 (2010).
30. Y. Meir, E. Jerby, *Microw. Opt. Technol. Lett.* **53**, 2281 (2011).